Experimental investigation on the effectiveness of MHTHS using different metal oxide-based nanofluids

G. Sriharan[1] · S. Harikrishnan[2] · H. M. Ali[3]

Abstract

In recent times, the mini heat sink is suggested for cooling the miniature components employed in several engineering applications. In the present work, the thermal performance of the mini hexagonal tube heat sink (MHTHS) was investigated experimentally. Nanofluids and deionized water (DIW) were made to flow through the hexagonal tube side and mini-passage side, respectively. For the preparation of different nanofluids of 0.01 volume fraction, DIW was considered to be a base fluid; Al_2O_3, CuO, and SiO_2 nanoparticles were reckoned to be the supporting materials. Experiments were run under two different conditions in order to ascertain the enhanced thermal performance of the MHTHS. They are as follows: (1) keeping the flow rate of hot DIW constant at 30 L h^{-1} in the mini-passage side, the flow rates of nanofluids in the hexagonal tube were varied such as 15, 20, 25, 30, 35, 40, 45, and 50 L h^{-1}; (2) keeping the flow rate of nanofluids constant at 30 L h^{-1} in the hexagonal tube side, the flow rates of hot DIW in the mini-passage side were varied such as 15, 20, 25, 30, 35, 40, 45, and 50 L h^{-1}. From the experimental results, it divulges that the heat transfer coefficient and effectiveness were found to be higher for Al_2O_3–DIW nanofluid, while comparing other nanofluids. A further improvement in the thermal performance of MHTHS could be achieved at higher volume flow rates of nanofluids in the hexagonal tube side and constant volume flow rate of hot DIW in the mini-passage side.

Keywords Mini hexagonal tube · Mini-passage · Heat sink · Nanofluids · Volume flow rate · Effectiveness

Introduction

The management of thermal energy is under demand, and it has to be properly handled since the components in the modernized system generate a larger amount of heat. More efforts are made to develop many techniques for recovering the heat where it is wasted or unutilized. Heat exchangers are widely used to capture the waste heat. However, they could harvest only limited quantity of heat, and it is mainly due to the flow of conventional fluid whose thermal conductivity and specific heat capacity are not higher. After the development of nanoscience and nanotechnology, a novel fluid was prepared by Choi, known as nanofluid [1]. If the solid nanoparticles are dispersed into base fluid, then it is said to be nanofluid. The thermal conductivity of nanofluids is found to be greater than that of the conventional fluids [2–6]. Nanofluids are passed to flow through the heat exchangers in order to study the improved performance of the heat exchangers. The entire effectiveness of the heat exchanger depends on the mass flow rate, volume concentration, viscosity, density, specific heat, and thermal conductivity of the nanofluid [7, 8]. Choi and Zhang [9] investigated that an increase in the volume fraction of nanoparticles causes decreases in the specific heat of nanofluid. Based on the past literature, it is observed that heat exchangers using nanofluids could be able to achieve improved heat transfer performance for a wide range of operating temperatures [10]. Also, many studies in the past reported that the heat transfer coefficient of heat exchangers using nanofluids is higher than the base fluid alone [11–13].

✉ S. Harikrishnan
   ramhkn@gmail.com

   H. M. Ali
   hafiz.ali@kfupm.edu.sa

[1] Department of Mechanical Engineering, AVC College of Engineering, Mannampandal, Mayiladuthurai, Tamilnadu, India

[2] Department of Mechanical Engineering, Kings Engineering College, Irungattukottai, Chennai, India

[3] Mechanical Engineering Department, King Fahd University of Petroleum and Minerals, Dhahran 31261, Saudi Arabia

Over the last decades, the microchannel heat sink was an essential method for extracting heat developed in numerous engineering applications. Tuckerman and Pease [14] were the first to propose and illustrate the fluid flow through the microchannels heat sink. They described that the microchannel cooling could be a useful strategy to dissipate the heat produced in electronic devices. Hetsroni et al. [15] conducted their research and initiated the performance in microchannel fluid flow and heat transfer. Fluid flowing through channels was represented as microchannels, and their hydraulic diameter is 0.5 mm or lesser. Harms et al. [16] carried out a study on a silicon heat sink. A typically lower Reynolds number prominently moves from laminar to turbulent flow, which was related to a sharp inlet of the channel, analogously a lengthy entry region, and channel surface roughness. Garg et al. [17] conducted a study in different shapes and geometries of the microchannel heat sink of various aspect ratios. It was examined that the heat transfer coefficient can be improved to 2.5 times the water than that of other fluids.

Rudyak et al. [18] demonstrated that the heat transfer coefficient of nanofluid depends on the volume concentration and size of the nanoparticles. The viscosity and the thermal conductivity of nanofluid increase with an increase in the particle size. The heat transfer coefficient can be determined by the flow patterns (laminar or turbulent flow) of nanofluid. The use of the nanofluid as a coolant influences the significance of the heat transfer coefficient. In the case of laminar flow, the heat transfer coefficient in nanofluid is high while comparing base fluid without nanoparticles, and also, it was reported that nanofluid increases the heat transfer coefficient by 2%. Chein and Chuang [19] evaluated the performance of microchannel with CuO/H_2O nanofluid. The result showed that nanofluid-based cooled microchannel absorbs higher energy than water-based cooled microchannel at higher flow rates. Husain and Kim [20] implemented the numerical investigation with trapezoidal microchannel heat sink. They have optimized design parameters such as depth, width, and fin width, with finite volume method using Navier–Stokes equation and energy equation. The result proved that optimization of shape promotes an increase in thermal performance with a subsequent decrease in thermal resistance by 12% from their standard shapes.

Salimpour et al. [21] investigated the optimization of numerical geometry of 3D microchannel with elliptical, rectangular, and isosceles triangular sections. The cross-sectional areas of these profiles were changed based on the volume fraction and aspect ratio. The results reveal that rectangle and elliptical cross sections were able to achieve the higher performance than isosceles triangular cross section. Khan and Kim [22] investigated the performance on hydraulic and thermal analysis in various seven geometry shapes of the microchannel heat sink using Navier–Stokes

equation, and it was compared with another microchannel of same diameter and height. Friction factor coefficient, Nusselt number, and thermal resistance were calculated under Reynolds number between 50 and 500. The result showed that inverse of trapezoidal shapes provides lower thermal resistance up to Reynolds number of 300. The values of Reynolds number were almost similar for the constant hydraulic diameter of all shapes.

Garg et al. [23] conducted experimental and numerical investigations on various shape geometry microchannels with a significant effect on different aspect ratios. The three different fluids, such as deionized water, ethylene glycol, and conventional nanofluid, were used to find friction factor, thermal resistance, and heat transfer coefficient. The result revealed that conventional nanofluid has a higher heat removal rate and better overall performance of the system. From the past literature, it was observed that heat transfer coefficient of heat sink using nanofluids is enhanced. If effectiveness is increased, there is an improvement in the performance of the system. There are a limited number of studies carried out on the function of nanofluids to improve the effectiveness in the mini and micro heat sinks. Based on the past literature, it is understood that it is yet to probe the heat transfer performance of mini-channel heat sink further. To the best of our knowledge, it is the first kind with the profile of mini hexagonal tube heat sink (MHTHS). Thus, the present study was experimentally investigated to ascertain the enhanced heat transfer coefficient and effectiveness using different nanofluids.

Methods and experiments

Preparation of nanofluids

The metal oxide nanoparticles such as CuO, Al_2O_3, and SiO_2 were purchased from Sigma-Aldrich Private Limited, India. The thermo-physical properties of nanoparticles are presented in Table 1. The size and morphology of nanoparticles were characterized using scanning electron microscopy (SEM) in Fig. 1a–c and transmission electron microscopy (TEM) in Fig. 2a–c, respectively. Nanofluids were prepared by adding three metal oxide nanoparticles with 0.01 volume fraction (VF) into DIW (base fluid, b_f), separately. Then, these three mixtures were stirred with the help of a magnetic stirrer for 8 h at 700 rpm, and this process could be useful to achieve uniform dispersion of nanoparticles in the base fluid. Afterward, the mixtures were undergone sonication process in order to warrant long-term dispersion stability. The thermo-physical properties of nanofluid are mentioned in Table 2.

Table 1 Thermo-physical properties of nanoparticles at 300 K

Nanoparticles	Size of nanoparticles/nm	Thermal conductivity/W m^{-1} K^{-1}	Specific heat/J kg^{-1} K^{-1}	Density/kg m^{-3}
CuO	40	33	533.1	6316
Al$_2$O$_3$	20	37	785.0	3892
SiO$_2$	50	2.2	745.8	2223
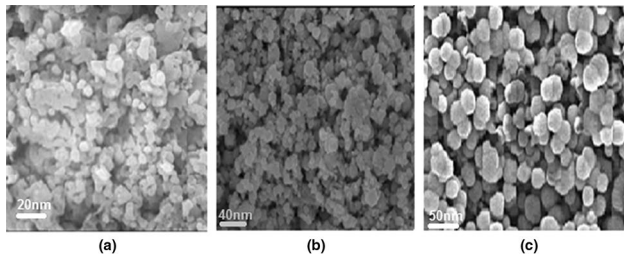
Fig. 1 SEM image of **a** Al$_2$O$_3$ nanoparticles, **b** CuO nanoparticles, **c** SiO$_2$ nanoparticles
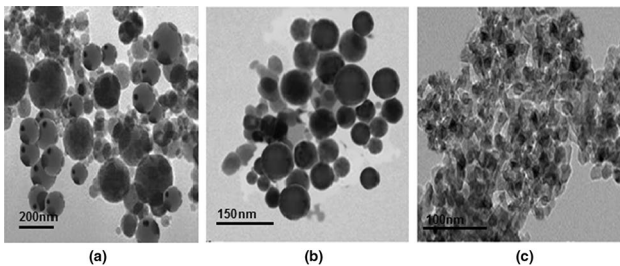

Fig. 2 TEM image of **a** Al$_2$O$_3$ nanoparticles, **b** CuO nanoparticles, **c** SiO$_2$ nanoparticles

Experimental setup

The MHTHS comprised three rows and five columns of the hexagonal tube having diameter and length of 0.5 cm and 5 cm, respectively. An oval-shaped slot was provided at the end of each row of tubes through which nanofluids can be allowed to flow within the hexagonal tube from inlet to exit. The hexagonal tube was arranged one above another, which provided the mini-passage between the hexagonal tubes, as shown in Fig. 3. The heater was placed in the DIW storage tank, and it can supply the heat to DIW at a desired temperature. The nanofluid and hot DIW were passed through the hexagonal tube and mini-passage with the help of a peristaltic pump (model: RH-P100L-100, Ravel Hiteks Pvt. Ltd.). The flow meters (PD flow meter, Flui-Tec Instruments and Control Pvt. Ltd.) were fitted at the flow paths of nanofluid and hot DIW, and the volume flow rate could be regulated by means of control valve. The schematic diagram and detailed view of the experimental setup are shown in Figs. 4 and 5, respectively. The J-type thermocouples (accuracy ± 2 °C, Tip Temperature Product Pvt. Ltd.) were connected at inlet and outlet pipes for nanofluids and base fluid. The inlet and outlet temperatures were monitored, and steady-state values were recorded for calculation purpose. The experiments were repeated for four times in order to ascertain the reliability of the measured data. Uncertainties of the measured parameters are given in Table 3.

Thermal conductivity measurements

The thermal conductivity of nanofluid was measured using KD2 Pro (Decagon Devices Inc.). The device consists of a needle sensor and a controller used to measure the thermal conductivity of fluid samples. KD2 Pro Instrument was calibrated with standard fluid of distilled water and glycerol, and it showed a maximum deviation of $\pm 0.5\%$ at 25°. The thermal conductivities of three nanofluids were measured at the temperature ranging from 40° to 60°, and measurements were repeated in a regular interval of 30 min, in order to ensure the accuracy of the measured data, and the resultant values were recorded. The relative uncertainty of the thermal conductivity was observed between 1.5 and 2.5%.

Viscosity measurements

The rheological stress and shear viscosity of nanofluid were determined using a rotation rheometer

Table 2 Thermo-physical properties of nanofluids at 300 K

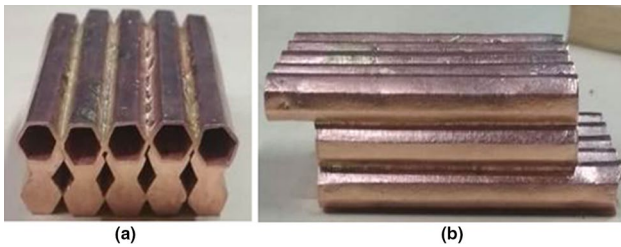| Nanofluids	Thermal conductivity/W m^{-1} K^{-1}	Specific heat/J kg^{-1} K^{-1}	Density/kg m^{-3}	Viscosity/kg m^{-1} s^{-1}
DIW	0.6171	4182.3	997.4	0.00092
Al$_2$O$_3$–DIW	0.6187	4180.7	998.3	0.00097
CuO–DIW	0.6185	4172.6	998.9	0.00099
SiO$_2$–DIW	0.6172	4179.2	997.6	0.00095

Fig. 3 Photographic image of inside skeleton **a** front view and **b** side view of hexagonal tube in MHTHS

(R/S-CC +/R/S-CPS +, R/S plus a controlled stress rheometer, AMETEK Brookfield). The viscosity of the nanofluid to be measured was filled in the concentric cylinder. The viscosity measurements were carried out at room temperature of 25°. The uncertainty in viscosity measurements was estimated as 2.5%.

Model calculations

Mini-passage side

The hydraulic diameter of the mini-passage D_{hmin} depends on the cross-sectional area of mini-passage A_{min} and the wetted perimeter of the mini-passage P_{min}. Subscript min indicates mini-passage. They are presented in Eqs. (1–3).

Fig. 5 Photographic image of experimental setup of MHTHS

$$D_{hmin} = \frac{4A_{min}}{P_{min}} \tag{1}$$

$$A_{min} = \frac{D_1 D_2}{2}. \tag{2}$$

$$P_{min} = 4a \tag{3}$$

Let D_1, D_2 determine the diagonal length of mini-passage, respectively, and a determines the side of the mini-passage.

The Reynolds number of base fluid R_{ebf} depends on ρ_{bf} as the density of the base fluid, u_m as mean base fluid velocity, D_{hmin} D_h as a hydraulic diameter of mini-passage, and μ_{bf} as the viscosity of the base fluid, and they are represented in Eq. (4).

$$R_{ebf} = \frac{\rho_{bf} u_m D_{hmin}}{\mu_{bf}}. \tag{4}$$

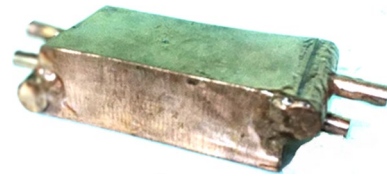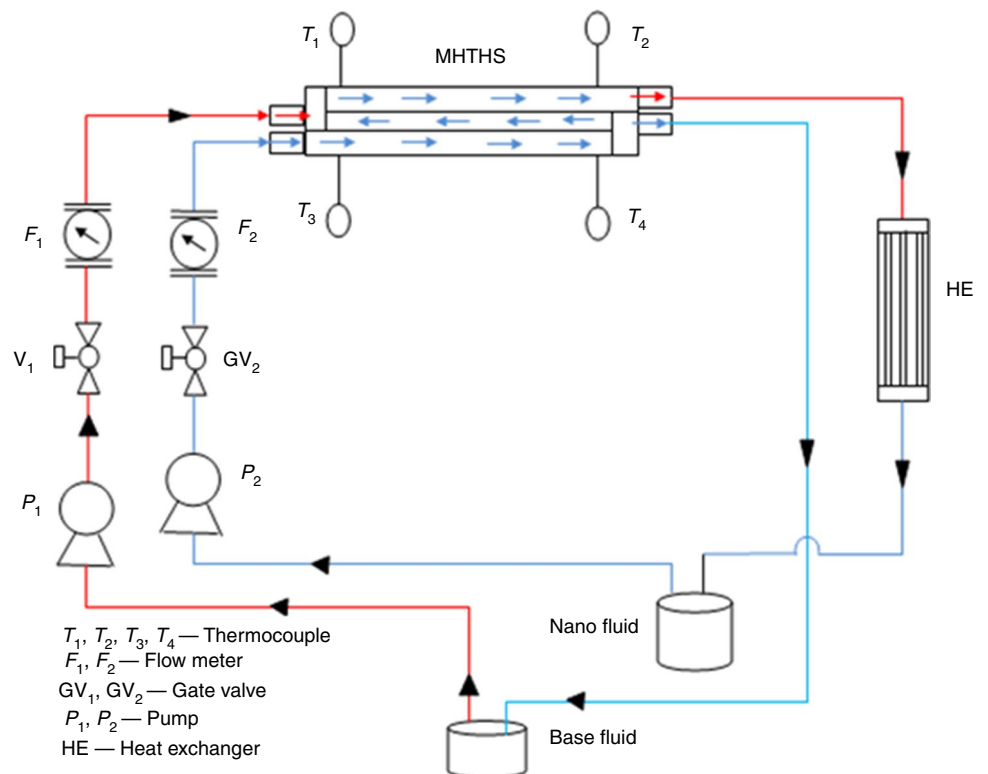**Fig. 4** Schematic diagram for MHTHS using various nanofluids

T_1, T_2, T_3, T_4 — Thermocouple
F_1, F_2 — Flow meter
GV_1, GV_2 — Gate valve
P_1, P_2 — Pump
HE — Heat exchanger

Prandtl number of the base fluid Pr_{bf} depends on the specific heat capacity of the base fluid Cp_{bf}, the viscosity of the base fluid μ_{bf}, and thermal conductivity of the base fluid K_{bf}, and Prandtl number is expressed in Eq. (5)

$$Pr_{bf} = \frac{c_{P_{bf}}\mu_{bf}}{K_{bf}}.$$ (5)

The heat transfer coefficient of the base fluid h_{bf} can be calculated by using Dittus–Boelter correlation in Eq. (6)

$$h_{bf} = \frac{0.36K_{bf}}{D_{hmin}}R_{e_{bf}}^{0.55}P_{r_{bf}}^{0.33}.$$ (6)

Hexagonal tube side

The hydraulic diameter of the hexagonal tube D_{hH} depends on the cross-sectional area of the hexagonal tube A_H and the wetted perimeter of hexagonal tube P_H. Side of the hexagonal tube a_H and subscript H denote hexagonal tube. The hydraulic diameter, cross-sectional area, and the wetted perimeter of hexagonal tube are determined by using Eqs. (7–9).

$$D_{hH} = \frac{4A_H}{P_H}$$ (7)

$$A_H = \frac{3\sqrt{3}}{2}a_H^2$$ (8)

$$P_H = 6a_H.$$ (9)

The Reynolds number of the nanofluid R_{enf} relies on the density of nanofluid ρ_{nf}, u_{mnf} as mean velocity of nanofluid, D_{hH} as a hydraulic diameter of the hexagonal tube, and μ_{nf} as a viscosity of the nanofluid, and they are presented in Eq. (10)

$$R_{enf} = \frac{\rho_{nf}u_{mnf}D_{hH}}{\mu_{nf}}.$$ (10)

Prandtl number of the nanofluid Pr_{nf} relies on the specific heat capacity of the nanofluid Cp_{nf}, the viscosity of the nanofluid μ_{nf}, and thermal conductivity of the nanofluid K_{nf}, and it can be found using Eq. (11).

Table 3 Uncertainties of the measured parameters

Parameter measured	Instrument	Uncertainty/%
Temperature	J-type thermocouple	± 1.2
Thermal conductivity	KD2 Pro analyzer	± 2.0
Viscosity	Rheometer	± 1.5
Velocity	PD flow meter	± 2.0

$$Pr_{nf} = \frac{c_{P_{nf}}\mu_{nf}}{K_{nf}}.$$ (11)

Nusselt number of the nanofluid Nu_{nf} represented by Reynolds number of nanofluid R_{enf} and Prandtl number of the nanofluid Pr_{nf} is given by Eq. (12).

$$Nu_{nf} = 0.024R_{enf}^{0.8}Pr_{nf}^{0.4}.$$ (12)

The heat transfer coefficient of the nanofluid h_{bf} can be determined by Nusselt number of the nanofluid Nu_{nf}, the thermal conductivity of nanofluid K_{nf}, and hydraulic diameter of the hexagonal tube D_{hH}, and it is given by Eq. (13).

$$h_{nf} = \frac{Nu_{nf}K_{nf}}{D_{h_H}}.$$ (13)

The density (ρ_{nf}) [24], thermal conductivity (K_{nf}) [25], viscosity (μ_{nf}) [26], and specific heat ($C_{P_{nf}}$) [27] of the nanofluid are obtained by using Eqs. (14–17).

$$\rho_{nf} = (1 - \emptyset)\rho_{bf} + \emptyset\rho_{np}$$ (14)

$$K_{nf} = \frac{K_{np} + (n-1)K_{bf} - (n-1)\emptyset(K_{bf} - K_{np})}{K_{np} + (n-1)K_{bf} + \emptyset(K_{bf} - K_{np})}K_{bf}$$ (15)

$$\mu_{nf} = \frac{1}{(1-\emptyset)^{2.5}}\mu_{bf}$$ (16)

$$(\rho C_{np})_{nf} = (1-\emptyset)(\rho C_p)_{bf} + \emptyset(\rho C_{np})_{np}$$ (17)

where ϕ represents the volume concentration of the nanoparticles, subscript nf determines nanofluid, and subscript np represents nanoparticles. 'n' indicates the number of hexagonal tubes in MHTHS, K_{np} represents thermal conductivity of nanoparticles, and ρ_{np} denotes the density of nanoparticles.

Effectiveness of the heat sink using nanofluid can be determined by using mass flow rate of the base fluid (m_{bf}) and nanofluid (m_{nf}). Let Cp_{bf} and Cp_{nf} represent the specific heat capacities of base fluid and nanofluid, respectively. $(mc_p)_{min}$ represents the minimum values of either $m_{nf}\,Cp_{nf}$ or $m_{bf}\,Cp_{bf}$. The inlet temperature of the base fluid is represented as T_{ibf}, the outlet temperature of the base fluid is represented as T_{obf}, and temperature at the inlet of nanofluid is represented as T_{inf}, and Eq. (18) is given as follows:

$$\varepsilon = \frac{m_{bf}C_{P_{bf}}[T_{i_{bf}} - T_{o_{bf}}]}{(mC_P)_{min}[T_{i_{bf}} - T_{i_{nf}}]}.$$ (18)

Results and discussion

Variation of flow rate in hexagonal tube side

The performance of MHTHS with respect to the volume flow rate of nanofluids was discussed in detail. In this case, the volume flow rates of nanofluids passing through hexagonal tube side were varied and the flow rate of hot DIW passing through mini-passage side was kept at a constant.

Effect of volume flow rate of nanofluid on the heat transfer coefficient

Variation of volume flow rate of the nanofluids on the heat transfer coefficient can be studied. By varying the volume flow rates of nanofluid in the hexagonal tube side and keeping constant volume flow rate of base fluid (DIW) in mini-passage side, the enhancement of heat transfer coefficient (h_{nf}) was assessed in the present work. From Fig. 6, it is observed that a higher heat transfer coefficient for all three nanofluids was achieved and, however, maximum enhancement was noticed in Al_2O_3–DIW nanofluid; minimum enhancement was found in SiO_2–DIW nanofluid. Due to higher thermal conductivity of Al_2O_3–DIW nanofluid (Table 2), it could accelerate the heat transfer over other two nanofluids, and consequently, it increases the heat transfer coefficient. Further, the thermal conductivity of SiO_2–DIW nanofluids was able to achieve lower enhancement compared to other two nanofluids. This is the reason why the heat transfer coefficient of SiO_2–DIW nanofluids was found to be low. Besides, as the flow rate of base fluid in the mini-passage was kept constant, the temperature at the wall surface could be expected to be constant. Then, the flow rate of nanofluid of higher thermal conductivity passing through the hexagonal tube could absorb the heat at a faster rate. Hence, it is clear evident that Al_2O_3–DIW nanofluid of higher thermal conductivity achieved the higher heat transfer coefficient while comparing CuO–DIW and SiO_2–DIW nanofluids.

Effect of volume flow rate of nanofluid on effectiveness

Despite the higher heat transfer coefficient, effectiveness plays a significant role in the performance of the heat sink. The increase in effectiveness of the heat sink was evaluated in terms of volume flow rate of nanofluids in the hexagonal tube side. The effectiveness of the heat sink is dependent on the thermal conductivity and the specific heat capacity. In Fig. 7, it is seen that Al_2O_3–DIW nanofluid showed higher effectiveness when compared with CuO–DIW and SiO_2–DIW nanofluid. As stated above, the higher thermal conductivity and the specific heat capacity of Al_2O_3–DIW nanofluid could be advantageous in improving

the effectiveness. The higher heat transfer is due to the higher thermal conductivity and specific heat of nanofluids, which increases the temperature of nanofluids that causes an increase in effectiveness. The enhanced thermal conductivity and specific capacity of Al_2O_3–DIW nanofluid were able to accelerate the heat transfer, and as a result, this improved heat transfer of the nanofluid which could be helpful to enhance the effectiveness.

Variation of flow rate in mini-passage side

In this section, the effect of the volume flow rate of DIW on the thermal performance of MHTHS was discussed. Here, flow rate of nanofluid in the hexagonal tube was kept constant, whereas the flow rate of DIW in the mini-passage side was varied.

Effect of volume flow rate of DIW on the heat transfer coefficient

It is observed from Fig. 8 that the heat transfer coefficients of Al_2O_3–DIW, CuO–DIW, and SiO_2–DIW nanofluids decrease with an increase in volume flow rate of hot DIW in the mini-passage side. It is due to the fact that an increase in volume flow rate of DIW in the mini-passage side could cause the wall temperature to decrease, and as a result, it could reduce the thermal diffusion rate of nanofluid. Though the thermal conductivity of Al_2O_3–DIW nanofluid has high thermal conductivity, it is not able to absorb heat from hot DIW at a faster rate. It might be because value of the temperature difference between nanofluid and DIW decreases and due to uneven temperature distribution at the wall surface at higher volume flow rate of DIW. Hence, it could deter the heat absorption from the hot DIW to nanofluid. The reduction in heat transfer rate could cause the heat transfer coefficient to decrease.
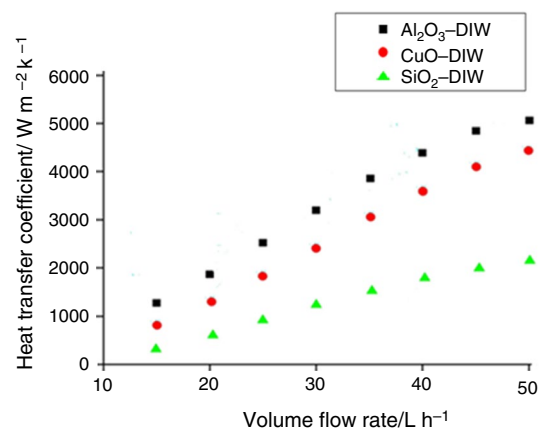
Fig. 6 Effect of volume flow rate of nanofluid on the heat transfer coefficient

Effect of volume flow rate of DIW on the effectiveness

In Fig. 9, the relationship between the effectiveness of nanofluids and the volume flow rate of base fluid is shown. Here, the volume flow rate of hot DIW was varied from 15 to 50 L h^{-1} and the effectiveness of Al$_2$O$_3$–DIW, CuO–DIW, and SiO$_2$–DIW nanofluids was determined. It can be observed from Fig. 9 that the effectiveness of nanofluids decreases with increases in volume flow rate of hot DIW. It is mainly due to drop in temperature difference and non-uniform temperature distribution at the wall surface. Also, as the volume flow rates of the nanofluids were kept constant, the effect of Brownian motion on nanofluid was lower. Consequently, it might cause the thermal diffusion to decrease, resulting in reduced effectiveness of nanofluids.

Enhancement of the heat transfer coefficient and effectiveness using nanofluids

The degrees of enhancement in the heat transfer coefficient and the effectiveness of three nanofluids prepared in the present work are presented in Figs. 10 and 11. The enhancement of heat transfer coefficients for Al$_2$O$_3$–DIW, CuO–DIW, and SiO$_2$–DIW nanofluids was 18.05%, 12.36%, and 6.50%, respectively. Based on the results, it can be inferred that the degree of enhancement in heat transfer coefficient relies on the thermal conductivity of the nanofluids, viscosity of the nanofluids and dispersion stability of the nanofluids. As far as the viscosity of the nanofluid is concerned, it could be as low as possible. Only then, nanofluid with less viscosity could promote the heat transfer at a faster rate as it would develop less friction while flowing. Also, if the dispersion stability of nanofluid is poor, then it could lead to aggregation, resulting in low thermal conductivity.
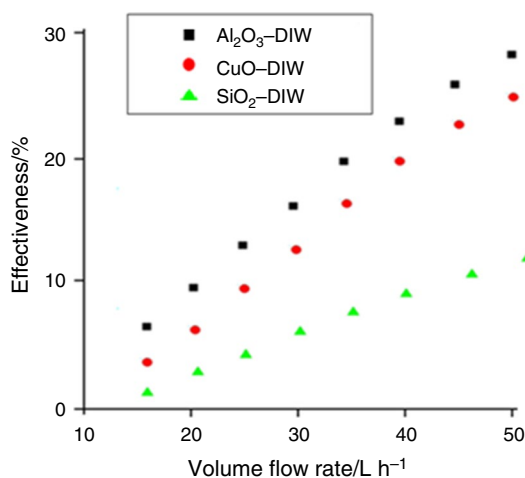
The effectiveness plays a significant role in assessing the performance of heat sink. From Fig. 11, it can be found that the enhancement of effectiveness for Al$_2$O$_3$–DIW, CuO–DIW, and SiO$_2$–DIW nanofluids was 29.67%, 24.03%, and 12.58%, respectively. As far as the present study is concerned, the effectiveness of the heat sink is dependent on the thermal conductivity, fluid flow resistance, specific heat capacity, and thermal resistance of the nanofluid. Based on the results, it can be understood that Al$_2$O$_3$–DIW nanofluid has higher thermal conductivity; SiO$_2$–DIW nanofluid has lower thermal resistance; and CuO–DIW has moderate thermal conductivity and thermal resistance. Finally, it can be concluded that to achieve higher enhancement of heat transfer coefficient and effectiveness, nanofluids of high thermal conductivity, low viscosity and thermal resistance are preferred.

Effect of volume flow rate of the nanofluids on the Nusselt number

In Fig. 12, the relationship between the volume flow rate and the Nusselt number of the nanofluids is shown. As we know, when the volume flow rate is increased, the velocity of the nanofluid is also increased. Subsequently, Reynolds number could be expected to increase which in turn would improve the heat transfer. As the Reynolds number increases, it causes increases in Nusselt number. Based on the results shown in Fig. 12, it is divulged that as the volume flow rate of nanofluid increases, Nusselt number also increases. An increase in Nusselt number is evaluated by the increase in heat transfer coefficient and Reynolds number. In the present work, the maximum enhancement of Nusselt number was observed in Al$_2$O$_3$–DIW nanofluid at higher Reynolds number. Also, according to Brownian motion, movement of nanoparticles nearer to the wall surface of the hexagonal

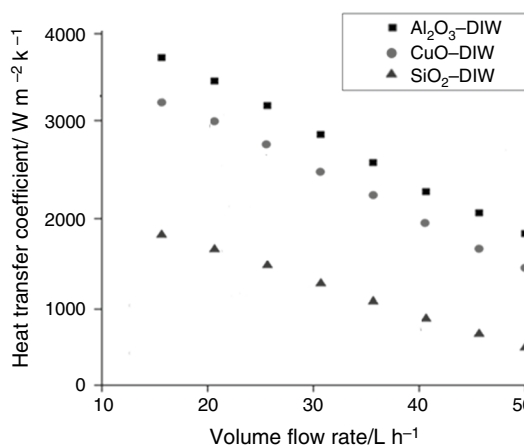**Fig. 7** Effect of volume flow rate of nanofluid on the effectiveness

Fig. 8 Effect of volume flow rate of DIW on the heat transfer coefficient
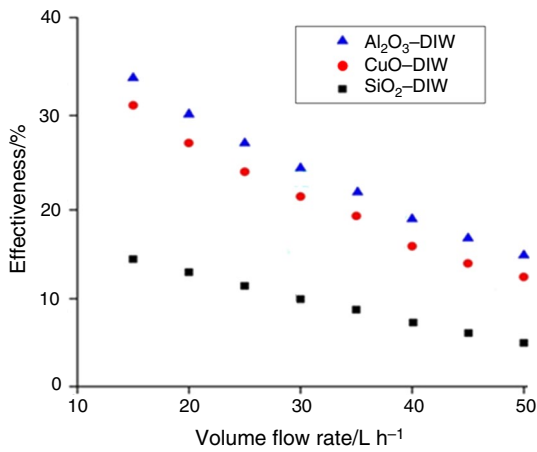
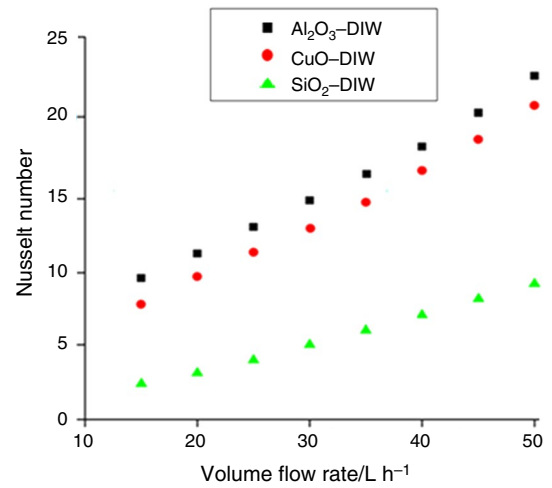**Fig. 9** Effect of volume flow rate of DIW on the effectiveness

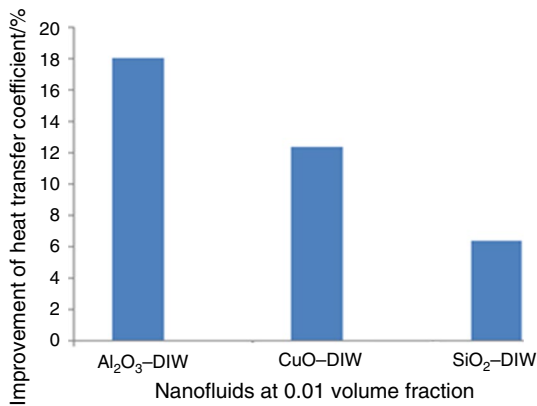**Fig. 12** Effect of volume flow rate of the nanofluids on the Nusselt number

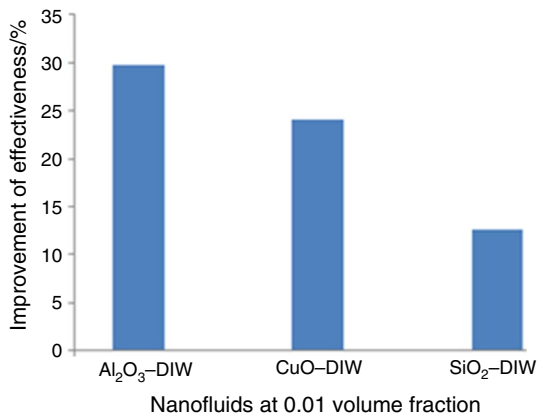**Fig. 10** Enhancement of the heat transfer coefficient using nanofluids

tube could expedite the heat transfer since the nanoparticles dispersed in DIW could increase the thermal conductivity of the base fluid. Further, an increase in Nusselt number was noticed in CuO–DIW and SiO$_2$–DIW nanofluids when the volume flow rate of the nanofluids was increased.

Effect of the volume flow rate of the nanofluids on the thermal resistance

The thermal resistances of nanofluids were studied with regard to the volume flow rate, and the results are shown in Fig. 13. The thermal resistance of the nanofluids relies on the density, the viscosity of nanofluid, and flocculation of nanoparticles. It shows that as the volume flow rates of the nanofluids increase, the thermal resistances of the nanofluids
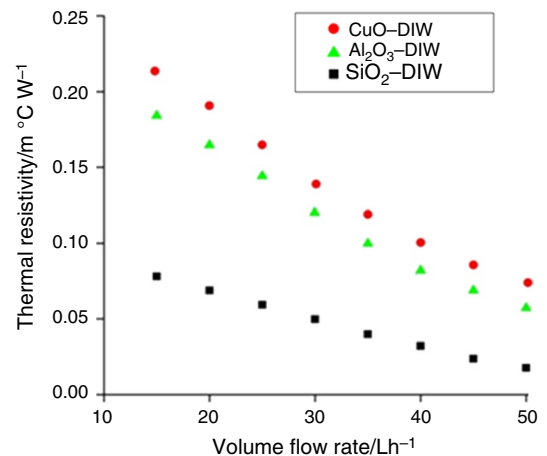

Fig. 11 Enhancement of the effectiveness using nanofluids

Fig. 13 Effect of the volume flow rate of the nanofluids on the thermal resistance

diminish. Figure 13 demonstrates that with decreasing thermal resistance, the thermal resistance of CuO–DIW nanofluid is found to be higher as compared to Al$_2$O$_3$–DIW, and SiO$_2$–DIW nanofluids. From Table 2, it is seen that CuO–DIW nanofluid has high density and viscosity. Also, CuO nanoparticles could aggregate at higher volume flow rates. The rise in thermal resistance of CuO–DIW nanofluid can be reduced by increasing the temperature of the nanofluid, and as a result, the viscosity of the nanofluid could be reduced, resulting in higher heat transfer rate. Furthermore, this increase in thermal resistance of nanofluid could make only negligible effect against heat transfer performance since the increase in thermal conductivity of the nanofluid is greater than that of the increase in thermal resistance.

Effect of the volume flow rate of the nanofluids on the pumping power

The pumping power for different nanofluids (CuO–DIW, Al$_2$O$_3$–DIW, and SiO$_2$–DIW) was determined with respect to the volume flow rate. The volume flow rate of the fluid is influenced by the density and the viscosity. Also, different morphologies of the nanoparticles could make a significant effect on the viscosity enhancement of the nanofluids [28]. Figure 14 elucidates that as the volume flow rate increases, the pumping power also increases. Test results presented in Fig. 14 display that the pumping power required for SiO$_2$–DIW nanofluid is low when compared with Al$_2$O$_3$–DIW and CuO–DIW nanofluids. It can be due to the low density and morphology of SiO$_2$ nanoparticles. When comparing pure DIW, the increase in pumping power for CuO–DIW, Al$_2$O$_3$–DIW, and SiO$_2$–DIW nanofluids was 3.6%, 3.2%, and 2.4%, respectively. As far as the heat transfer performance of MHTHS is concerned, this rise in the pumping power of nanofluids can be negligible, and further,
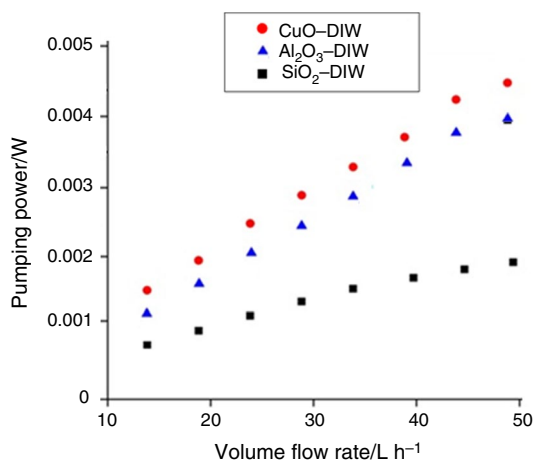
it would never introduce any adverse effect against the performance of the MHTHS.

Conclusions

The present work demonstrates that the effectiveness of MHTHS could be improved using different metal oxide-based nanofluids. Al$_2$O$_3$–DIW nanofluid was able to achieve enhanced effectiveness while comparing CuO–DIW and SiO$_2$–DIW nanofluids. The heat transfer coefficient was found to be higher for Al$_2$O$_3$–DIW nanofluid. At higher volume flow rates, the Nusselt number for Al$_2$O$_3$–DIW nanofluid was determined to be high when compared with CuO–DIW and SiO$_2$–DIW nanofluids. When comparing Al$_2$O$_3$–DIW and SiO$_2$–DIW nanofluids, the thermal resistance of CuO–DIW nanofluid was found to be high, and it could be decreased while increasing the volume flow rate of nanofluids. In order to realize the improved thermal performance of MHTHS, the volume flow rate of the base fluid in mini-passage side must be kept constant, and the volume flow rate of nanofluids in the hexagonal tube side can be varied.

References

1. Choi SUS, Siginer DA, Wang HP. Enhancing thermal conductivity of fluids with nanoparticles in developments applications of non-Newtonian flows. ASME. 1995;66:99–105.
2. Murshed SMS, Leong KC, Yang C. Enhanced thermal conductivity of TiO$_2$–water based nanofluids. Int J Therm Sci. 2005;44:367–73.
3. Yiamsawasd T, Dalkilic AS, Wongwises S. Measurement of the thermal conductivity of titania and alumina nanofluids. Thermochim Acta. 2012;545:48–56.
4. Lee SW, Park SD, Kang S, Bang IC. Kim JH Investigation of viscosity and thermal conductivity of SiC nanofluids for heat transfer applications. Int J Heat Mass Transf. 2011;54:433–8.
5. Harikrishnan S, Magesh S, Kalaiselvam S. Preparation and thermal energy storage behaviour of stearic acid–TiO$_2$ nanofluids as a phase change material for solar heating systems. Thermochim Acta. 2013;565:137–45.
6. Harikrishnan S, Roseline AA, Kalaiselvam S. Preparation and thermo physical properties of water-glycerol mixture-based CuO nanofluids as PCM for cooling applications. IEEE Trans Nanotechnol. 2013;12(4):629–35.
7. Keblinski P, Eastman JA, Cahill DG. Nanofluids for thermal transport. Mater Today. 2005;8:36–44.
8. Mahbubul IM, Fadhilah SA, Saidur R, Leong KY, Amalina MA. Thermo physical properties and heat transfer performance of Al$_2$O$_3$/R134 a nano refrigerants. Int J Heat Mass Transf. 2013;57:100–8.
9. Choi J, Zhang Y. Numerical simulation of laminar forced convection heat transfer of Al$_2$O$_3$–water nanofluid in a pipe with return bend. Int J Therm Sci. 2012;55:90–102.
10. Chein R, Huang G. Analysis of micro channel heat sink performance using nanofluids. Appl Therm Eng. 2005;25:3104–14.

Fig. 14 Effect of the volume flow rate of the nanofluids on the pumping power

11. Xuan Y, Li Q. Heat transfer enhancement of nanofluids. Int J Heat Fluid Flow. 2000;21:58–64.

12. Li Q, Xuan Y. Experimental investigation on convective heat transfer of nanofluids. J Eng Thermophys. 2002;23:721–3.

13. Liu Fang, Cai Yang, Wang Liqiu, Zhao Jun. Effects of nanoparticles shape on laminar forced convective heat transfer in curved ducts using two-phase model. Int J Heat Mass Transf. 2018;116:292–305.

14. Tuckerman DB, Pease RFW. High performance heat sinking for VLSI. IEEE Electron Device Lett. 1981;2:126–9.

15. Hetsroni G, Mosyak A, Pogrebnyak E, Yarin LP. Fluid flow in micro channels. Int J Heat Mass Transf. 2005;48:1982–98.

16. Harms TM, Kazmierczak MJ, Cerner FM, Holke A, Henderson HT, Pilchowski J, Baker K. Experimental investigation of heat transfer and pressure drop through deep micro channels in a (1 0 0) silicon substrate. Proc ASME Heat Transf Div. 1997;351:347–57.

17. Garg H, Negi VS, Garg N, Lall A. Numerical and experimental analysis of micro channel heat transfer for nanoliquid coolant using different shapes and geometries. Proc Inst Mech Eng Part C J Mech Eng Sci. 2014;229:2056–65.

18. Rudyak VY, Minakov AV. Thermo physical properties of nanofluids. Eur Phys J E. 2018;41:15.

19. Chein R, Chuang J. Experimental micro channel heat sink performance studies using nanofluids. Int J Therm Sci. 2007;46:57–66.

20. Husain A, Kim KY. Thermal optimization of a micro channel heat sink with trapezoidal cross section. J Electron Packag. 2009;131:021-005.

21. Salimpour MR, Sharifhasan M, Shirani E. Constructal optimization of micro channel heat sinks with noncircular cross sections. Heat Transf Eng. 2013;34:863–74.

22. Khan AA, Kim KY. Evaluation of various channel shapes of a micro channel heat sink. Int J Air-Cond Refrig. 2016;24:165018.

23. Garg H, Negi VS, Garg N, Lall A. Numerical and experimental analysis of micro channel heat transfer for nanoliquid coolant using different shapes and geometries. Proc Inst Mech Eng Part C J Mech Eng Sci. 2015;229:2056–65.

24. Drew DA, Passman SL. Theory of multicomponent fluids, vol. 1351. Berlin: Springer; 1999. p. 308.

25. Hamilton RL, Crosser OK. Thermal conductivity of heterogeneous two component systems. Ind Eng Chem Fundam. 1962;1:182–91.

26. Brinkman HC. The viscosity of concentrated suspensions and solutions. J Chem Phys. 1952;20:571–81.

27. Yang SM, Tao WQ. Heat transfer. 3rd ed. China: Higher Education Press Beijing; 1998.

28. Harikrishnan S, Deepak K, Kalaiselvam S. Thermal energy storage behavior of composite using hybrid nanomaterials as PCM for solar heating systems. J Therm Anal Calorim. 2013;115:1563–71.